

Thermal stability of vapor phase deposited self-assembled monolayers for MEMS anti-stiction

Yan Xin Zhuang¹, Ole Hansen¹, Thomas Knieling^{2,5},
Christian Wang³, Pirmin Rombach³, Walter Lang²,
Wolfgang Benecke², Markus Kehlenbeck^{4,6} and Jörn Koblitz⁴

¹ CINF, MIC-Department of Micro and Nanotechnology, Technical University of Denmark, Building 345 east, DK-2800, Kgs. Lyngby, Denmark

² Institute for Microsensors, -actuators and -systems (IMSAS), University of Bremen, Bibliothekstraße 1, D-28359 Bremen, Germany

³ Sonion MEMS A/S, Byleddet 12-14, DK-4000, Roskilde, Denmark

⁴ microFAB Bremen GmbH, Universitaetsallee 5, D-28359 Bremen, Germany

E-mail: yz@mic.dtu.dk and oh@mic.dtu.dk

Received 6 July 2006, in final form 14 August 2006

Published 12 September 2006

Online at stacks.iop.org/JMM/16/2259

Abstract

Six different source chemicals (organosilanes) were successfully used for deposition of self-assembled monolayers (SAMs) onto silicon substrates by a vapor phase process. Five different fluorocarbon coatings and one hydrocarbon coating were deposited. The thermal stability of the coatings was studied in detail with respect to degradation as a function of temperature, and for the fluorocarbon coatings also the degradation rate at 400 °C. For fluorocarbon coatings deposited from FDTS a useful lifetime of approximately 90 min at 400 °C was found allowing the coating to survive high temperature MEMS packaging operations, while fluorocarbon coatings deposited from FOTS, FOMDS, FOTES and FOMMS were less stable. The hydrocarbon coating deposited from OTS degrades already at approximately 200 °C. The thermal stability of the SAM coatings was found to be significantly reduced if aggregations from the deposition process are present on the coatings.

1. Introduction

Stiction is a serious problem in microelectromechanical systems (MEMS) due to the larger surface area to volume ratio, and significantly affects the efficiency, reliability, lifetime and manufacturing yield of MEMS devices [1–8]. Stiction can occur during fabrication (release stiction) and/or operation (in-use stiction). During the last few years, much effort has been devoted to solving stiction problems [9–19]. In-use stiction related failure is a major problem and will be increasingly important with continued miniaturization toward nanoscale structures. Deposition of a thin film

with low surface energy on microstructures is an efficient method to avoid or reduce in-use stiction problems. Among various surface coatings and modification techniques, self-assembled monolayers (SAMs) formed from organosilanes are promising anti-stiction coatings due to their good bonding strength, low surface energy, low friction forces and good thermal stability. Self-assembled monolayers can be deposited either in a liquid phase process or in a vapor phase process. Liquid phase deposition of SAM coatings has significant disadvantages, such as complicated process control, generation of large amounts of contaminated effluents, insufficient stiction prevention and high production costs. Vapor phase SAM deposition can eliminate some drawbacks of liquid-based SAM deposition, and thereby attract strong attention [17, 18].

⁵ Current address: Fraunhofer Institute of Photonic Microsystems, Marie-Reiche-Strasse 2, D-01109 Dresden, Germany.

⁶ Current address: Hella Fahrzeugkomponenten GmbH, D-28133 Bremen, Germany.

Six SAM coatings formed from various organosilanes have been successfully deposited on the silicon substrate in a vapor phase process [19]. The six chemicals have two different surface terminal groups (trifluoromethyl $-\text{CF}_3$ and methyl $-\text{CH}_3$), three different spacer chains ($-(\text{CF}_2)_7(\text{CH}_2)_2-$, $-(\text{CF}_2)_5(\text{CH}_2)_2-$ and $-(\text{CH}_2)_{17}-$) and four different surface active head groups (trichlorosilane $-\text{SiCl}_3$, methylchlorosilane $-\text{Si}(\text{CH}_3)\text{Cl}_2$, dimethylchlorosilane $-\text{Si}(\text{CH}_3)_2\text{Cl}$ and triethoxysilane $-\text{Si}(\text{OC}_2\text{H}_5)_3$), which react with the surface to form a strong chemical bond. The reaction mechanism is described in [20] where it is stated that the type of bonds formed depends strongly on the type of the head group and its functionality, e.g. chlorine (functional) or methyl (nonfunctional rest). Only trifunctional silanes are able to form monolayers which are strongly linked together by Si–O–Si-bonds. This results in high stability against external impact, especially against thermal influence. Trifunctional silanes are most reactive; thus the reaction time is expected to be comparatively low. Monofunctional silanes are only able to form covalent bonds, and difunctional silanes form covalent bonds or vertical polymerizations. The resulting layers are expected to be loosely packed and rougher than the monolayer assembly due to oligomerization. Moreover the thermal stability is expected to be weaker than for layers grown from trifunctional silanes.

Well-deposited coatings have good anti-stiction properties, such as high water contact angle ($>110^\circ$) and low adhesion force. On the other hand, the thermal stability of the coatings is very important when considering subsequent packaging processes, for long-term durability of coated devices, and for coatings used on stamps for nanoimprint processes. In this work, the thermal stability of the SAM coatings is studied in detail with respect to degradation temperatures, lifetime at high temperature (400°C) and the effect of aggregations.

2. Experimental techniques

Six different organosilanes were used for vapor phase deposited self-assembled monolayer (SAM) coatings. They are tridecafluoro-1,1,2,2-tetrahydrooctyl trichlorosilane $\text{CF}_3(\text{CF}_2)_5(\text{CH}_2)_2\text{SiCl}_3$ (FOTS), tridecafluoro-1,1,2,2-tetrahydrooctyl triethoxysilane $\text{CF}_3(\text{CF}_2)_5(\text{CH}_2)_2\text{Si}(\text{OC}_2\text{H}_5)_3$ (FOTES), tridecafluoro-1,1,2,2-tetrahydrooctyl methylchlorosilane $\text{CF}_3(\text{CF}_2)_5(\text{CH}_2)_2\text{Si}(\text{CH}_3)\text{Cl}_2$ (FOMDS), tridecafluoro-1,1,2,2-tetrahydrooctyl dimethylchlorosilane $\text{CF}_3(\text{CF}_2)_5(\text{CH}_2)_2\text{Si}(\text{CH}_3)_2\text{Cl}$ (FOMMS), heptadecafluoro-1,1,2,2-tetrahydrodecyl trichlorosilane $\text{CF}_3(\text{CF}_2)_7(\text{CH}_2)_2\text{SiCl}_3$ (FDTS) and n-octadecyltrichlorosilane $\text{CH}_3(\text{CH}_2)_{17}\text{SiCl}_3$ (OTS). The self-assembled monolayers were deposited onto monosilicon (100) substrates by the vapor phase coating setup described in [19]. Before the actual coating process, a pretreatment step was applied in order to terminate the monosilicon wafer surface with OH groups. The pretreatment step comprises a treatment in an O_2 -plasma for 30 min in a Tepla barrel reactor at 100 W, a Piranha clean ($\text{H}_2\text{O}_2:\text{H}_2\text{SO}_4$, 1:1) at 100°C for 15 min, followed by quick dump rinse in DI water and smooth nitrogen brush drying at low temperature. Then the silicon wafer was loaded into the process chamber together with Petri dishes containing precursors. After

heating and a reduction of the pressure to 0.2 mbar, the silane precursor evaporates into the inner process chamber space and creates a saturated atmosphere consisting of the coating molecules which react on the substrate and form an SAM coating.

Contact angle measurements were performed with contact angle meter DSA10 from Krüss GmbH equipped with an automatic dispensing system for four liquids and a frame grabber. Static contact angles were used to evaluate the quality and thermal stability of SAM coatings. The static contact angle values were taken 5 s after deposition of the droplets on the surface to allow droplet relaxation. At least ten measurements were performed on each droplet and the static contact angle values reported are the average of measurements on at least ten droplets. The surface energy of the coatings was calculated from static contact angles according to the Owens–Wendt–Rabel–Kaelble method as described in [6].

The micro topography and roughness of the SAM coatings were investigated using a commercial AFM (NanoMan, Digital Instruments, USA) in tapping mode with commercial silicon tips. The images were analyzed using the software Nanoscope 6.12 (Digital Instruments, USA). The roughness of coatings is characterized by the average roughness (R_a) and the root mean square (R_{RMS}) roughness. All roughness data are based on a $5 \times 5 \mu\text{m}^2$ scanning area in order to eliminate the scanning length effect.

In addition, water condensation figures were investigated in some cases in order to study the coating homogeneity. For this purpose, the sample to be studied was sealed in a transparent box together with a water droplet and cooled by a Peltier element. Water condensates on the cooled surface and the resulting condensation figures were recorded by a CCD camera mounted on a microscope.

For the thermal stability studies, the SAM coatings were heated to a specified temperature on a hotplate for a given time in air. The samples were then removed from the hotplate to a bulk aluminum plate and allowed to cool down to room temperature. Afterwards the static water contact angles were measured at room temperature.

3. Results and discussions

SAM coatings were deposited in a vapor phase process [19] from the source chemicals FDTS, FOTS, FOMMS, FOMDS, FOTES and OTS. AFM was used to check the quality of the deposited coatings e.g. to determine if aggregations were present on the coated surfaces. The static water contact angle (θ_{st}), surface energy (γ_{sv}), root mean square roughness (R_{RMS}) and average roughness (R_a) of the SAM coatings used in figures 1 and 4 are listed in table 1, where the data for the coatings are ordered according to increasing total surface energy. There are no or only a few aggregations on those SAM coatings as observed in AFM. However, wafers with many aggregations were also produced with other less appropriate process parameters.

Figure 1 shows the static water contact angle of the FDTS, FOTS, FOMMS, FOMDS, FOTES and OTS as a function of annealing temperature, when the samples were sequentially annealed for 2 min at each temperature. Since aggregations on the coating affect the thermal stability of the

Table 1. Static water contact angles, total surface energy and the dispersive and polar surface energy contributions and roughness of the six SAM coatings on silicon.

	FDTS	FOTS	FOMDS	FOTES	FOMMS	OTS
θ_{st} (water) ^a	115.4	107.6	106.0	103.6	104.3	100.0
Surface energy γ_{sv} (mJ m ⁻²)	9.95	13.22	13.38	14.26	14.9	25.44
γ_{sv} dispersive component (mJ m ⁻²)	9.06	11.45	11.08	11.56	12.29	24.65
γ_{sv} polar component (mJ m ⁻²)	0.89	1.77	2.30	2.70	2.61	0.79
R_{RMS} (nm) ^b	0.18	0.09	0.22	0.15	0.22	0.11
R_a roughness (nm) ^b	0.14	0.07	0.13	0.12	0.12	0.09

^a The static water contact angle of the silicon substrate is around 20°.

^b R_{RMS} and R_a roughness of the uncoated silicon substrate are 0.34 and 0.28 nm, respectively.

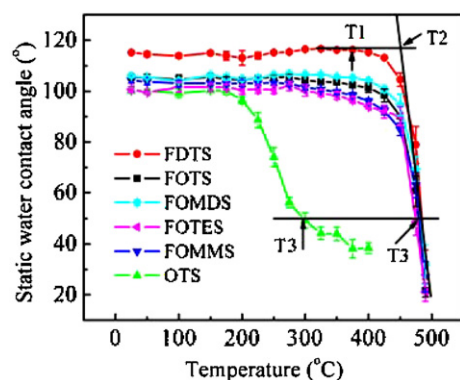


Figure 1. The static water contact angle as a function of annealing temperature for six SAM coatings grown from FDTS, FOTS, FOMDS, FOTES, FOMMS and OTS. The samples were sequentially annealed for 2 min on a hotplate at each temperature.

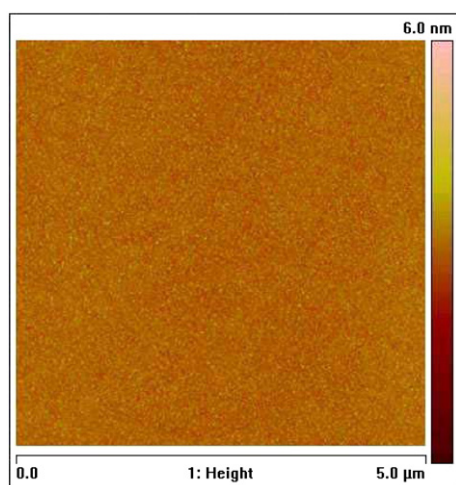


Figure 2. Tapping mode AFM image of a FDTS coating, showing a high quality coating without observable aggregations.

coating (see the text below), the samples used in figure 1 are those without aggregations as verified by tapping mode AFM images. One of such AFM images is shown in figure 2. From figure 1 it is seen that OTS degrades at much lower temperature than the fluorinated coatings; already at 180 °C the water contact angle of OTS is reduced by the thermal treatment due to its hydrocarbon backbone. The five different fluorinated coatings have quite similar degradation behavior and their static water contact angles are only slightly affected at temperatures below 450 °C. In order to characterize the

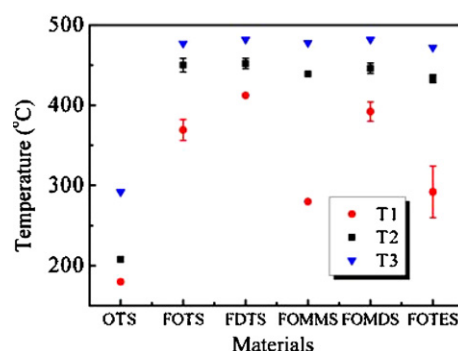


Figure 3. Degradation temperatures T_1 , T_2 and T_3 for the six SAM coatings. FDTS, FOTS and FOMDS have better thermal stability than FOTES, FOMMS and OTS.

thermal degradation behavior three characteristic temperatures are defined, T_1 is the temperature where the static water contact angle starts to decrease, T_2 is the temperature corresponding to the intersection of the two tangents of the zero and the negative slope part of the curves and finally T_3 is the temperature where the static contact angle has degraded to a threshold value (here 50°). Figure 3 shows these degradation temperatures for the six coatings. Even though the five fluorinated coatings have similar values of T_2 , which is above 425 °C, and T_3 , which is roughly 480 °C, FOMMS and FOTES have lower values of T_1 , which is below 300 °C. This might be caused by an incomplete reaction between the functional group of the organosilane and the substrate, possibly caused by steric hindrance due to the large substituents close to their functional group, leading to weak bonding of a fraction of the coating. Also FOTS and FOMDS seem to show such effects, but much less pronounced. FDTS has the best thermal stability followed by FOTS and FOMDS which also show very good thermal stability.

Figure 4 displays the static water contact angle for the five fluorinated SAM coatings as a function of annealing time at an annealing temperature of 400 °C on a hotplate in air. For each curve, only a single sample is used, i.e. after getting one measurement point, the sample is reheated at the same temperature (400 °C) for another defined time, and then the contact angle is measured and recorded. The static water contact angles of all the five SAM coatings decrease with time. It can be seen that the thermal stability decreases in the order of FDTS, FOMDS, FOTS, FOTES and FOMMS for the samples investigated, which is in agreement with the order of the initial surface energy of the SAM coatings (see table 1). The thermal stability might be different for coatings grown

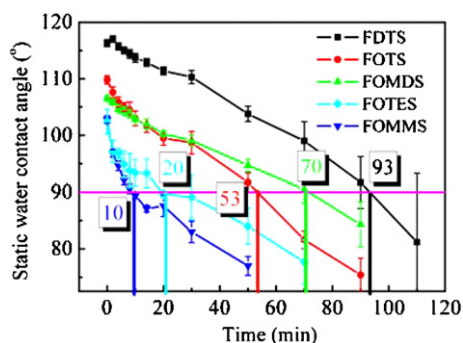


Figure 4. The static water contact angle as a function of anneal time at 400 °C for the fluorinated SAM coatings grown from FDTS, FOTS, FOMDS, FOMMS and FOTES. The labels show the lifetime in minutes at a 90° threshold contact angle.

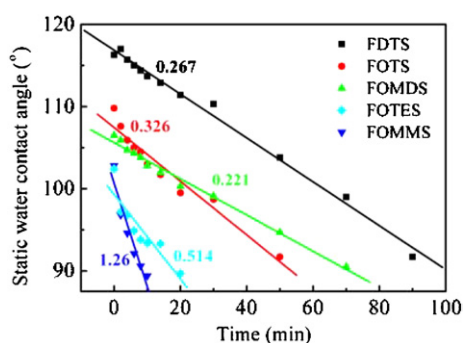


Figure 5. The initial degradation rate at 400 °C for the five fluorinated SAM coatings. FDTS, FOTS and FOMDS degrade slowly at approximately the same rate, while FOMMS and FOTES degrade at a much higher rate.

from the same source chemical but with a different coating quality (see the text below). If 90° is defined as the threshold contact angle, below which the coating loses its hydrophobic properties for practical applications, the lifetime at 400 °C is 93 min for FDTS, 70 min for FOMDS, 53 min for FOTS, 20 min for FOTES and 10 min for FOMMS. It can also be observed that the static water contact angle is almost linearly dependent on the annealing time when the contact angle is larger than 90°. The degradation rate, which is the slope of a linear fit to the data points in figure 4, is shown in figure 5. The initial degradation rate is 0.27° min⁻¹ for FDTS, 0.33° min⁻¹ for FOTS, 0.22° min⁻¹ for FOMDS, 0.51° min⁻¹ for FOTES and 1.26° min⁻¹ for FOMMS. The degradation is slow for FDTS, FOMDS and FOTS, while the degradation of FOTES and FOMMS is much faster again probably due to weak bonding to the coated surface of part of the coating. Comparatively fast degradation for the first few data points is also seen for FOTS and FOMDS.

In order to investigate the effect of aggregations on the thermal stability of coatings, samples from three wafers coated with FOTS (A, B and C) were annealed at 400 °C and 380 °C, respectively. The three otherwise identical wafers were produced at different coating process parameters (e.g., significantly prolonged coating time for samples B and C), and thereby they have different coating qualities. Tapping mode AFM images and roughness of the three wafers are

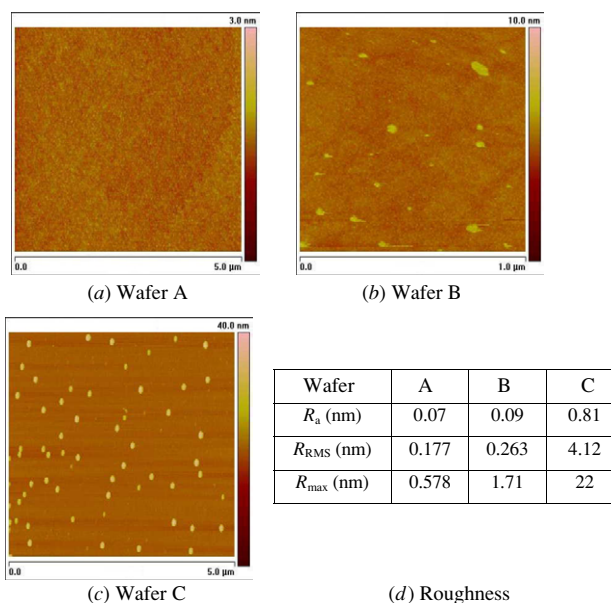


Figure 6. Tapping mode AFM images (a)–(c) and roughness (d) of three wafers coated using FOTS. Wafer A has no, wafer B a few and wafer C many aggregations. In (a) and (c) a 5 × 5 μm² scan area is shown, while (b) shows a 1 × 1 μm² scan area.

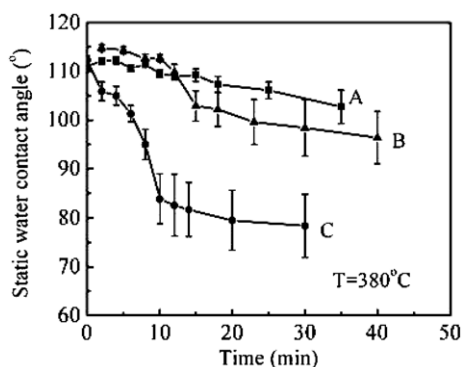


Figure 7. Thermal stabilities at 380 °C of three wafers coated with FOTS, showing that coatings with aggregations have poor thermal stability.

shown in figure 6. There are no aggregations on wafer A, a few aggregations on wafer B and many big aggregations (the maximum roughness is 22 nm) on wafer C. Figure 7 shows the static water contact angle as a function of annealing time at 380 °C for the three coatings. Obviously, the three samples have different thermal stabilities, which decrease in the order of samples A, B and C. It can be concluded from figures 6 and 7 that there is a correlation between surface aggregations and thermal stability. Coatings with aggregations initially degrade fast and thus have poor thermal stability. The same trend has been found at 400 °C. Aggregations are formed during the deposition process due to polymerization among molecules. Too much water vapor in the deposition chamber can induce polymerization of silane molecules, which then deposit onto the microstructures and form aggregations on the surface. This may also cause stiction or inhibit motion when applied to real devices. The coatings with aggregations are supposed to have partially poor coverage of

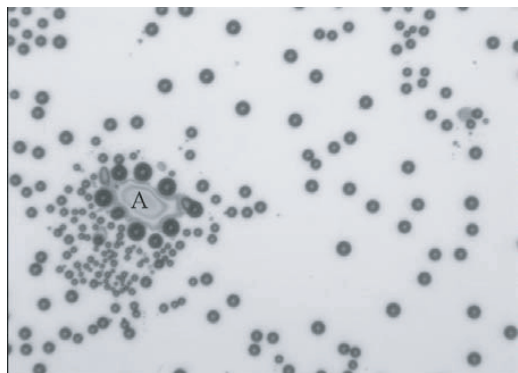


Figure 8. Water condensation figure of a FOTES sample, showing that the area surrounding the aggregation is more hydrophilic than other areas. The area marked as A is an aggregation formed in the coating deposition process.

the SAM coating, especially in areas close to the aggregations. Water condensation figures can be used to image such surface inhomogeneities. Lopez and co-workers reported that water preferentially condenses on hydrophilic areas of patterned SAMs, providing a sensitive probe of differences in interfacial free energies between localized areas [21]. Figure 8 shows a water condensation figure of a FOTES SAM coating, where aggregations were formed during the deposition process. Obviously, more water microdroplets have been formed in areas close to the aggregations, indicating that these areas are more hydrophilic than the aggregation itself and other areas. Therefore, areas close to the aggregation are not well covered by fluorocarbon chains, and these areas are supposed to be responsible for the poor thermal stability. de Boer and coworkers have also found [22] that a number of tall mounds are formed on samples exposed to high relative humidity (RH) after deposition. These mounds are formed due to restructuring of the surface monolayer rendering the surrounding area hydrophilic while the mound itself remains hydrophobic.

4. Conclusions

The thermal stability of self-assembled monolayer coatings grown from FOTS, FDTS, FOMDS, FOMMS, FOTES and OTS has been investigated in detail. The fluorocarbon coatings are far more stable than the hydrocarbon coating grown from OTS. Among the fluorocarbon coatings, coatings grown from FDTS have the best thermal stability. Coatings grown from FDTS have a useful lifetime of approximately 90 min at 400 °C, and are thus able to withstand post-deposition heat treatments in usual packaging operations. Aggregations found on poor quality deposited coatings significantly reduce the thermal stability of the coatings.

Acknowledgments

Financial support from the European Commission under contract G1ST-CT-2002-50354 is acknowledged. Y X Zhuang would like to thank the Danish Research Council for Technology and Production Sciences for financial support.

The center for Individual Nanoparticle Functionality (CINF) is sponsored by The Danish National Research Foundation. This paper is also in memory of Professor Aric Menon.

References

- [1] Bhushan B 2004 *Handbook of Nanotechnology* (Berlin: Springer)
- [2] Maboudian R and Howe R T 1997 Critical review: adhesion in surface micromechanical structures *J. Vac. Sci. Technol. B* **15** 1–20
- [3] Tas N, Sonnenberg T, Jansen H, Legtenberg R and Elwenspoek M 1996 Stiction in surface micromachining *J. Micromech. Microeng.* **6** 385–97
- [4] Komvopoulos K 2003 Adhesion and friction forces in microelectromechanical systems: mechanisms, measurement, surface modification techniques, and adhesion theory *J. Adhes. Sci. Technol.* **17** 477–517
- [5] Mastrangelo C H 1997 Adhesion-related failure mechanisms in micromechanical devices *Tribol. Lett.* **3** 223–38
- [6] Zhuang Y X and Menon A 2005 On the stiction of MEMS materials *Tribol. Lett.* **19** 111–7
- [7] Maboudian R 1998 Surface processes in MEMS technology *Surf. Sci. Rep.* **30** 207–69
- [8] Arney S 2001 Designing for MEMS reliability *MRS Bull.* **26** 296
- [9] Anguita J and Briones F 1998 HF/H₂O vapor etching of SiO₂ sacrificial layer for large-area surface-micromachined membranes *Sensor Actuators A* **64** 247–51
- [10] Guckel H, Sniegowski J J, Christenson T R and Raissi F 1990 The application of fine-grained, tensile polysilicon to mechanically resonant transducers *Sensors Actuators A* **21–23** 346–51
- [11] Mulhern G T, Soane D S and Howe R T 1993 *Proc. 7th Int. Conf. on Solid-State Sensors and Actuators—Transducers'93* p 296
- [12] Brzoska J B, Azouz I B and Rondelez F 1994 Silanization of solid substrates: a step toward reproducibility *Langmuir* **10** 4367–73
- [13] Srinivasan U, Houston M R, Howe R T and Maboudian R 1998 Alkyltrichlorosilane-based self-assembled monolayer films for stiction reduction in silicon micromachines *J. Microelectromech. Syst.* **7** 252–60
- [14] Maboudian R, Ashurt W R and Carraro C 2000 Self-assembled monolayers as anti-stiction coatings for MEMS: characteristics and recent developments *Sensors Actuators A* **82** 219–23
- [15] Ashurst W R, Yau C, Carraro C, Maboudian R and Dugger M T 2001 Dichlorodimethylsilane as an anti-stiction monolayer for MEMS: a comparison to the octadecyltrichlorosilane self-assembled monolayer *J. Microelectromech. Syst.* **10** 41–9
- [16] Kushmerick J G, Hankins M G, de Boer M P, Clews P J, Carpick R W and Bunker B C 2001 The influence of coating structure on micromachine stiction *Tribol. Lett.* **10** 103–8
- [17] Mayer T M, de Boer M P, Shinn N D, Clews P J and Michalske T A 2000 Chemical vapour deposition of fluoroalkylsilane monolayer films for adhesion control in microelectromechanical systems *J. Vac. Sci. Technol. B* **18** 2433–9
- [18] Ashurst W R, Carraro C and Maboudian R 2003 Vapor phase anti-stiction coatings for MEMS *IEEE Trans. Devices Mater. Reliab.* **3** 173–8
- [19] Knieling T 2006 Mikrosystemtechnisch hergestellte zweidimensionale Fabry-Perot-Interferenz displays zur einfachen Musterprojektion, Hydrophobisierung von Si-Mikrostrukturen aus der Gasphase *PhD Thesis* in preparation

- [20] Fadeev A Y and McCarthy T J 2000 Self-assembly is not the only reaction possible between alkyltrichlorosilanes and surfaces: monomolecular and oligomeric covalently attached layers of dichloro- and trichloroalkylsilanes on silicon *Langmuir* **16** 7268–74
- [21] Lopez G P, Biebuyck H A, Frisbie C D and Whitesides G M 1993 *Science* **260** 647
- [22] de Boer M P, Knapp J A, Michalske T A, Srinivasan U and Maboudian R 2000 Adhesion hysteresis of silane coated microcantilevers *Acta Mater.* **48** 4531–41